

measurements in Au+Au collisions at $\sqrt{s_{NN}} = 200$ GeV with the STAR experiment

著者 (英)	STAR Collaboration, Shinichi ESUMI
journal or publication title	Nuclear physics. A
volume	982
page range	723-726
year	2019-02
権利	(C) 2018 Published by Elsevier B.V. This is an open access article under the CC BY-NC-ND license (http://creativecommons.org/licenses/by-nc-nd/4.0/).
URL	http://hdl.handle.net/2241/00157823

doi: 10.1016/j.nuclphysa.2018.09.025



XXVIIth International Conference on Ultrarelativistic Nucleus-Nucleus Collisions
(Quark Matter 2018)

Υ measurements in Au+Au collisions at $\sqrt{s_{NN}} = 200$ GeV with the STAR experiment

Pengfei Wang (for the STAR Collaboration)^{a,b}

^aUniversity of Science and Technology of China, Hefei 230000, China

^bBrookhaven National Laboratory, Upton, NY 11973, USA

Abstract

We present the latest measurements of Υ production in Au+Au collisions at $\sqrt{s_{NN}} = 200$ GeV via both di-muon and di-electron decay channels by the STAR experiment at RHIC. With the addition of the 2016 data set to those taken in 2011 and 2014, the precision of Υ measurements is significantly improved compared to previous preliminary results, especially for the excited Υ states. The nuclear modification factors for the ground and excited Υ states are shown as a functions of transverse momentum or centrality, and are compared to results from the LHC as well as to theoretical calculations.

Keywords:

Color screening, Dissociation, Upsilon, Suppression, STAR

1. Introduction

Measurements of quarkonium production play an important role in understanding the properties of the Quark-Gluon Plasma (QGP) created in relativistic heavy-ion collisions. J/ψ suppression in the medium due to the color screening effect was proposed as a direct signature of the QGP formation [1]. Moreover, different quarkonium states may dissociate at different temperatures due to different binding energies [2], and thus measurement of this so-called “sequential melting” can help constrain the thermodynamic properties of the medium. However, other effects, such as cold nuclear matter (CNM) effects and regeneration, need to be taken into account when interpreting the experimental results on quarkonium suppression in heavy-ion collisions. Compared to charmonia, the bottomonia Υ states are a cleaner probe at the RHIC collision energies: 1) the regeneration contribution is smaller compared to J/ψ due to the much smaller $b\bar{b}$ production cross section than the $c\bar{c}$ [3, 4]; 2) the cross section for inelastic interactions between $\Upsilon(1S)$ and other hadrons is small, hence the co-mover absorption is predicted to be minimal [5]. However, the Υ measurements are statistically challenging at RHIC and require dedicated triggers to sample large amounts of luminosities.

The Υ production has been studied at RHIC in different collision systems via the di-electron decay channel, including p+p, d+Au and Au+Au collisions at $\sqrt{s_{NN}} = 200$ GeV [6] and U+U collisions at $\sqrt{s_{NN}} = 193$ GeV [7]. In this article, we present the combined results via the di-electron channel using 2011 data and the di-muon channel using 2014 and 2016 data.

2. Detector and data sample

The Solenoidal Tracker At RHIC (STAR) [8, 9] can reconstruct Υ from both the di-electron and di-muon decay channels. The Time Projection Chamber (TPC) is used in track reconstruction and precise momentum measurement with full azimuthal coverage over the pseudorapidity range $|\eta| < 1$. It also measures the ionization energy loss for particle identification. The Barrel Electromagnetic Calorimeter (BEMC) is used to identify and trigger on electrons with high transverse momenta (p_T) within $0 < \phi < 2\pi$ and $|\eta| < 1$. The Muon Telescope Detector (MTD) [10], which has been fully installed since 2014 and covers about 45% in azimuth within $|\eta| < 0.5$, is designed to identify and trigger on muons with high p_T . Compared to electrons, muons have less bremsstrahlung, which can facilitate the separation of excited Υ states from the ground state. The BEMC trigger in 2011 run and the MTD trigger in 2014 and 2016 runs sampled 1.1 nb^{-1} , 14.2 nb^{-1} and 12.8 nb^{-1} , respectively.

3. Results

3.1. Υ reconstruction

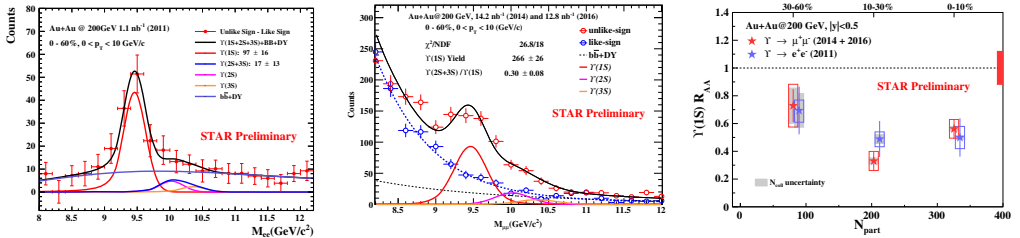


Fig. 1: Left: invariant mass distribution of Υ candidates (unlike-sign electron pair distribution with like-sign distribution subtracted) reconstructed via the di-electron channel. Middle: invariant mass distribution of Υ candidates reconstructed via the di-muon channel, where the unlike-sign distribution is fitted with Υ , $b\bar{b}$ and Drell-Yan templates from simulation and the combinatorial background is determined by fitting the like-sign distribution. Right: $\Upsilon(1S) R_{AA}$ from di-electron (blue) and di-muon (red) channels are shown as a function of N_{part} for $p_T > 0 \text{ GeV}/c$. The statistical and systematic uncertainties are shown as vertical bars and open boxes. The light grey band around each marker represents the uncertainty on N_{coll} . The red band at unity on the right side shows the global uncertainty from the p+p reference [11].

The invariant mass distribution of Υ candidates reconstructed via the di-electron channel is shown in the left panel of Fig. 1. The signal distribution (red circles) is obtained by subtracting the distribution of like-sign electron pairs from the unlike-sign one. It is then fitted with three crystal ball functions representing the three Υ states respectively, as well as a polynomial function describing the residual background from $b\bar{b}$ and Drell-Yan processes. The middle panel of Fig. 1 shows the invariant mass distributions of unlike-sign (red circles) and like-sign (blue circles) muon pairs. The like-sign distribution is used as an estimate of the combinatorial background, and is fitted with an exponential function whose parameters are fed into the fitting of the unlike-sign distribution. The unlike-sign distribution is fitted with templates from simulation for both the Υ signals and the residual background. For both the di-electron and di-muon channels, the excited Υ states are taken as a whole, and the relative abundance of $\Upsilon(2S)$ and $\Upsilon(3S)$ is fixed to the world-wide value [12].

3.2. Υ suppression

Since the measured nuclear modification factors (R_{AA}) of $\Upsilon(1S)$ and $\Upsilon(2S+3S)$ are consistent between the di-electron and di-muon channels (see the right panel of Fig. 1), they are combined to further increase the precision. In the left panel of Fig. 2, the $\Upsilon(1S)$ and $\Upsilon(2S+3S) R_{AA}$ in Au+Au collisions at $\sqrt{s_{NN}} = 200 \text{ GeV}$ are shown as a function of number of participants (N_{part}) using the p+p reference measured with

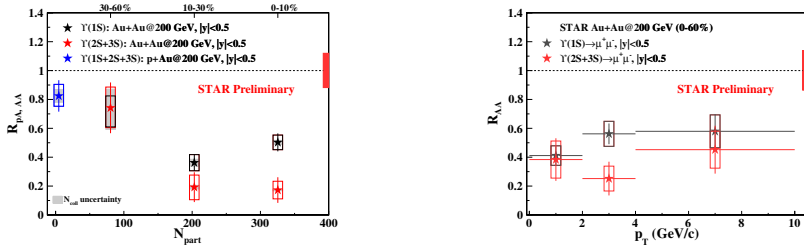


Fig. 2: Left: $\Upsilon(1S)$ (black) and $\Upsilon(2S+3S)$ (red) R_{AA} combined from di-electron and di-muon channels are shown as a function of N_{part} for $p_T > 0$ GeV/c. The R_{pA} of $\Upsilon(1S+2S+3S)$ for $|y| < 0.5$ measured through the di-electron channel is shown as the blue star. Right: $\Upsilon(1S)$ and $\Upsilon(2S+3S)$ R_{AA} as a function of p_T in 0-60% Au+Au collisions at $\sqrt{s_{NN}} = 200$ GeV. The red band at unity includes the uncertainties from p+p reference and N_{coll} .

2015 data through the di-electron channel [11]. For comparison, R_{pA} of $\Upsilon(1S+2S+3S)$ measured via the di-electron channel in 200 GeV p+Au collisions is also shown [11]. The suppression of $\Upsilon(2S+3S)$ in peripheral Au+Au collisions is comparable to the $\Upsilon(1S+2S+3S)$ suppression observed in p+Au collisions, and gets larger towards more central collisions. The suppression of $\Upsilon(1S)$ shows a similar trend. Compared to $\Upsilon(1S)$, $\Upsilon(2S+3S)$ is more suppressed in the 0-10% most central collisions, which is consistent with the sequential melting scenario. In the right panel of Fig. 2, $\Upsilon(1S)$ and $\Upsilon(2S+3S)$ R_{AA} measured via the di-muon channel are shown as a function of p_T . No significant p_T dependence is observed.

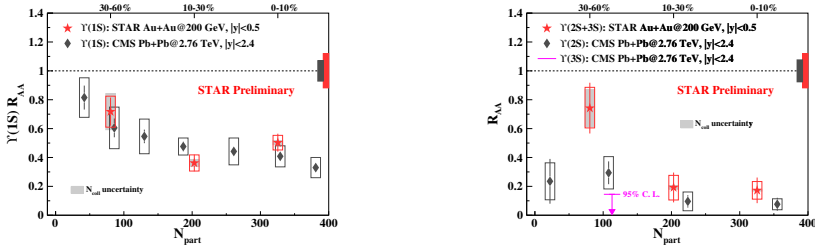


Fig. 3: Left: comparison of $\Upsilon(1S)$ R_{AA} for Au+Au collisions at $\sqrt{s_{NN}} = 200$ GeV (red stars) from STAR and for Pb+Pb collisions at $\sqrt{s_{NN}} = 2.76$ TeV (grey diamonds) from CMS [13]. The red and grey bands at unity show the global uncertainties for the STAR and CMS measurements, respectively. Right: comparison of excited states R_{AA} between STAR and CMS measurements.

The STAR results are compared to similar measurements by the CMS experiment at the LHC in Pb+Pb collisions at $\sqrt{s_{NN}} = 2.76$ TeV [13]. In the left panel of Fig. 3, one can see that the $\Upsilon(1S)$ suppression is similar between RHIC and the LHC. It is plausible that the suppression of inclusive $\Upsilon(1S)$ arises mainly from the CNM effects as well as the suppression of excited states that feed down to $\Upsilon(1S)$, while the direct $\Upsilon(1S)$ remains largely unaffected by the QGP in both 200 GeV Au+Au and 2.76 TeV Pb+Pb collisions. On the other hand, the $\Upsilon(2S+3S)$ seems to be less suppressed at RHIC than at the LHC, especially in peripheral collisions as shown in the right panel of Fig. 3.

Υ measurements at RHIC are also compared to two model calculations, which are shown in Fig. 4. The model of Krouppa, Rothkopf and Strickland [14] uses a lattice-vetted heavy-quark potential with an initial temperature of about 440 MeV for the QGP in most central collisions. The model of Du, He and Rapp [4] employs in-medium binding energies predicted by thermodynamic T-matrix calculations using internal-energy potentials from lattice QCD. The initial temperature of the QGP is about 310 MeV in the most central collisions. The regeneration and CNM effects are only included in the Rapp model. Both model calculations are consistent with experimental data within experimental and theoretical uncertainties.

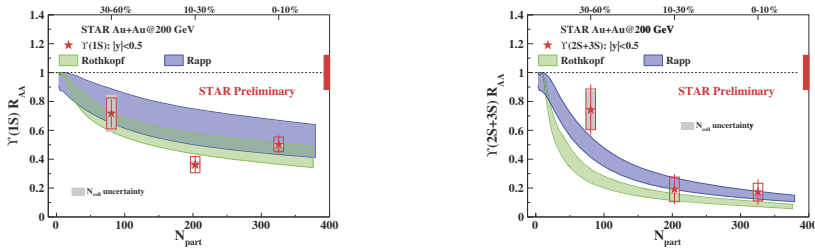


Fig. 4: Left: $\Upsilon(1S) R_{AA}$ compared to different model calculations. Right: $\Upsilon(2S+3S) R_{AA}$ compared to different model calculations.

4. Summary

We present the latest Υ measurements in Au+Au collisions at $\sqrt{s_{NN}} = 200$ GeV via both the di-electron and di-muon channels with the STAR experiment. The $\Upsilon(1S) R_{AA}$ as a function of centrality has a similar suppression as observed in Pb+Pb collisions at $\sqrt{s_{NN}} = 2.76$ TeV with no significant p_T dependence in 0-60% centrality class. $\Upsilon(2S+3S)$ is more suppressed than $\Upsilon(1S)$ in 0-10% most central collisions, which is consistent with the sequential melting picture. Two theory models, both incorporating different dissociation temperatures for different Υ states, are consistent with the experimental measurements.

Acknowledgments

We thank the RHIC Operations Group and RCF at BNL. P. Wang is supported by the China Scholarship Council (CSC). This work was supported in part by the Ministry of Science and Technology (MOST) of China under grant No. 2016YFE0104800, National Natural Science Foundation of China (NSFC) under Grants No. 11675168 and 11505180.

References

- [1] T. Matsui, H. Satz, J/ψ Suppression by Quark-Gluon Plasma Formation, Phys. Lett. B 178 (1986) 416–422. doi:10.1016/0370-2693(86)91404-8.
- [2] A. Mocsy, Potential models for quarkonia, Eur. Phys. J. C 61 (4) (2009) 705–710.
- [3] A. Emerick, X. Zhao, R. Rapp, Bottomonia in the quark-gluon plasma and their production at RHIC and LHC, Eur. Phys. J. A 48 (5) (2012) 72.
- [4] X. Du, M. He, R. Rapp, Color screening and regeneration of bottomonia in high-energy heavy-ion collisions, Phys. Rev. C 96 (2017) 054901. doi:10.1103/PhysRevC.96.054901.
- [5] Z. Lin, C. Ko, Υ absorption in hadronic matter, Phys. Lett. B 503 (1-2) (2001) 104–112.
- [6] L. Adamczyk, et al., (STAR Collaboration), Suppression of Υ production in d+ Au and Au+ Au collisions at $\sqrt{s_{NN}} = 200$ GeV, Phys. Lett. B 735 (2014) 127–137.
- [7] L. Adamczyk, et al., (STAR Collaboration), Υ production in U + U collisions at $\sqrt{s_{NN}} = 193$ GeV measured with the STAR experiment, Phys. Rev. C 94 (2016) 064904. doi:10.1103/PhysRevC.94.064904.
- [8] M. Harrison, S. Peggs, T. Roser, The RHIC Accelerator, Annu. Rev. Nucl. Part. Sci. 52 (1) (2002) 425–469.
- [9] K. Ackermann, et al., (STAR Collaboration), STAR Detector Overview, Nucl. Instrum. Meth. A 499 (2) (2003) 624–632.
- [10] T. C. Huang, et al., Muon Identification with Muon Telescope Detector at the STAR Experiment, Nucl. Instrum. Meth. A 833 (2016) 88–93. arXiv:1601.02910, doi:10.1016/j.nima.2016.07.024.
- [11] Z. Ye (for the STAR Collaboration), Υ measurements in p+ p, p+ Au and Au+ Au collisions at $\sqrt{s_{NN}} = 200$ GeV with the STAR experiment, Nucl. Phys. A 967 (2017) 600–603.
- [12] W. Zha, C. Yang, B. Huang, L. Ruan, S. Yang, Z. Tang, Z. Xu, Systematic study of the experimental measurements on ratios of different Υ states, Phys. Rev. C 88 (2013) 067901. doi:10.1103/PhysRevC.88.067901.
- [13] V. Khachatryan, et al., (CMS Collaboration), Suppression of $\Upsilon(1S)$, $\Upsilon(2S)$, and $\Upsilon(3S)$ quarkonium states in Pb+Pb collisions at $\sqrt{s_{NN}} = 2.76$ TeV, Phys. Lett. B 770 (2017) 357–379.
- [14] B. Krouppa, A. Rothkopf, M. Strickland, Bottomonium suppression using a lattice QCD vetted potential, Phys. Rev. D 97 (2018) 016017. doi:10.1103/PhysRevD.97.016017.